

# RSC Advances



This is an *Accepted Manuscript*, which has been through the Royal Society of Chemistry peer review process and has been accepted for publication.

*Accepted Manuscripts* are published online shortly after acceptance, before technical editing, formatting and proof reading. Using this free service, authors can make their results available to the community, in citable form, before we publish the edited article. This *Accepted Manuscript* will be replaced by the edited, formatted and paginated article as soon as this is available.

You can find more information about *Accepted Manuscripts* in the [Information for Authors](#).

Please note that technical editing may introduce minor changes to the text and/or graphics, which may alter content. The journal's standard [Terms & Conditions](#) and the [Ethical guidelines](#) still apply. In no event shall the Royal Society of Chemistry be held responsible for any errors or omissions in this *Accepted Manuscript* or any consequences arising from the use of any information it contains.



Journal Name

COMMUNICATION

## A novel route for preparation of Mn-containing hollow framework TS-1, and its selective allylic oxidation of cyclohexene

Received 00th January 20xx,  
Accepted 00th January 20xx

DOI: 10.1039/x0xx00000x

www.rsc.org/

Guoqiang Zou, Dai Jing, Wenzhou Zhong\*, Feiping Zhao, Liqiu Mao, Qiong Xu, Jiafu Xiao, Dulin Yin\*

**A new manganese-containing hollow framework TS-1 (MTS-1) was prepared via simple recrystallization of an traditional TS-1 in the presence of tetrapropylammonium hydroxide (TPAOH) and manganese(III)-acetylacetonate, and their catalytic performance was tested for aerobic oxidation of cyclohexene without any solvents. This hollow bimetal TS-1 catalysts are more active than catalysts containing Mn or Ti solely, the formation of metal framework sites may be responsible for increased activity. The characterization techniques such as UV-vis, FT-IR, Raman, XRD, N<sub>2</sub>-adsorption, TEM, and XPS can confirm the incorporation of Mn and Ti in the zeolite framework sites. This hollow catalyst shows highly catalytic activity and stability (ten cycles) in the oxidation of cyclohexene, and demonstrates the potential of TS-1 catalysts usable for aerobic oxidations.**

The oxidation of cyclic olefin, represented by cyclohexene, produces a variety of oxygen-containing derivatives. For example, 2-cyclohexene-1-ol and 2-cyclohexene-1-one are important intermediates in the spice industry and organic synthesis.<sup>1</sup> Recently, a variety of studies on the oxidation of cyclohexene by transition metal complexes have been reported in the literatures.<sup>2-4</sup> Although there have been some achievements, the search for more stable and efficient catalysts is never-ending.<sup>5,6</sup>

Zeolites with uniform and small pore size, high internal surface area, and flexible frameworks are widely used in heterogeneous catalysis fields.<sup>7</sup> The only presence of micropores, however, imposes restrictions on the reactions involving reactants or larger products whose size is approximate to the diameter of micropore. Under this conditions, mass transport to and from the active sites located within the micropores would be slow, greatly limiting the catalytic

performance of the zeolite catalysts.<sup>8</sup> Many efforts to overcome this difficulty, titanasilicate molecular sieves (TS-1), with MFI cages connected by 10-ring pore openings, have been developed.<sup>9,10</sup> They are well known for their excellent selective oxidation activity of organic molecules such as olefins, hydroxylation of aromatics in chemical industry.<sup>11</sup> The difficulty of large molecules transport within such microporous channels, however, is still existed.<sup>12</sup> In contrast, large-pore aluminophosphate molecular sieves and Ti-MCM were anticipated to overcome these diffusion and transport problems for the oxidation of bulky molecules. Due to the presence of Brønsted acid sites associated with framework aluminum and their low hydrothermal stability, it is difficult for them to displace TS-1 in industrial chemistry.<sup>13,14</sup>

In this communication, we synthesized a new hollow framework manganese-containing MFI-type zeolite (Scheme S1), which exhibited an excellent activity in the allylic liquid-phase oxidation of cyclohexene by using oxygen as oxidant without any solvent. Such a good performance in the catalytic activity of the catalyst might be ascribed to the framework Mn and Ti species as an excellent oxygen carrier and donor in the zeolite framework and bonded to the surface.<sup>15</sup> Furthermore, this solvent-free/dioxygen system as well as the stable crystalline structure of MTS-1 can suppress the leaching of active metal ion during heterogeneous reaction.

The UV-vis spectra of the prepared sample are shown in Fig. 1A. The pure silicate-1 and MnO<sub>x</sub> have no absorption in the range of 200–800 nm, while two absorption bands, at 250 and 515 nm, have been found in Mn-doped silicate-1. The band at 250 nm is ascribed to electron transfer from O<sup>2-</sup> to tetrahedral Mn<sup>3+</sup>, and the one close to 515 nm is attributed to d-d transition of either framework or possibly surface-associated Mn<sup>3+</sup>.<sup>16,17</sup> Obviously, the band centered at 210 nm shown in Fig. 1A was observed for manganese-free hollow framework titanasilicate (HTS-1), as reported by Wang et al.<sup>18</sup> This band is similar to the reported UV-vis spectra of traditional TS-1, which could be ascribed to the charge transfer from O<sup>2-</sup> to Ti<sup>4+</sup>, indicating the presence of tetrahedral Ti(IV) coordination species in the framework.<sup>19</sup> Another band at 330 nm was also appeared, reflecting most likely the presence of ex-framework Ti species.<sup>20</sup> Compared with the reference HTS-1, the prepared MTS-1

National & Local United Engineering Laboratory for New Petrochemical Materials & Fine Utilization of Resources, Hunan Normal University, Changsha 410081, P. R. China Tel & Fax: +86-731-8872576  
E-mail: zwenz79@163.com; dulinyin@126.com  
Electronic Supplementary Information (ESI) available: experiment section, the design idea of catalyst, the XRD and UV-vis spectra of the reused catalyst. See DOI: 10.1039/x0xx00000x

displayed a wide absorption band at 350–550 nm, which might be attributed to the overlap of the d–d transition framework  $Mn^{3+}$  and the ex-framework Ti species, or the metal-to-metal charge-transfer transition resulting from the overlap of  $Ti(e_g)$  and  $Mn(t_{2g})$  3d orbitals according to spectroscopic analysis of mixed metal minerals.<sup>21,22</sup>

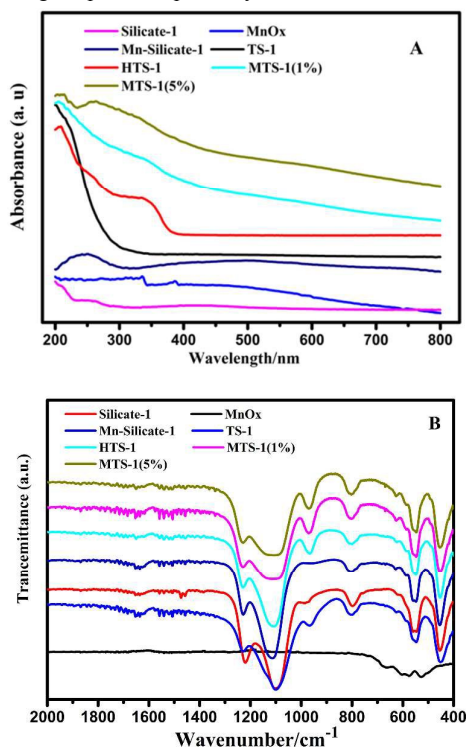


Fig. 1 UV-vis spectra (A) and FT-IR spectra (B) of the prepared catalysts

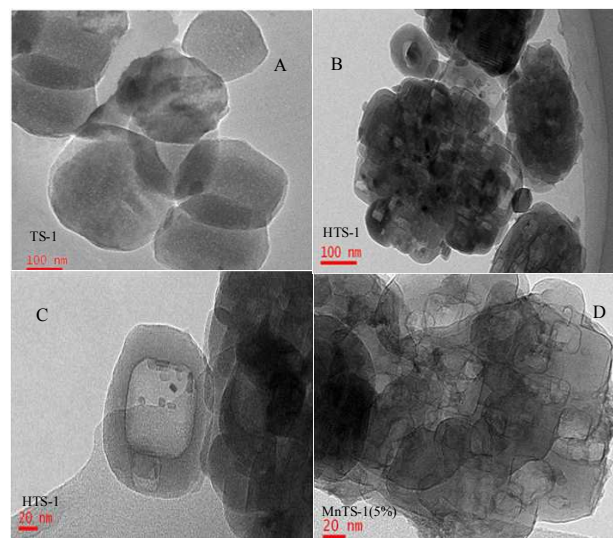


Fig. 2 TEM of the as-prepared catalysts

The characteristic vibration peaks found in the infrared spectra (Fig. 1B) inferred that the catalysts possess a typical structure of

MFI-type zeolite. The peak at  $550\text{ cm}^{-1}$  is typically due to the pentasil framework variation, which is used as a standard of the crystallinity of this type of material. The absorption peak at  $800\text{ cm}^{-1}$  is due to Si–O–Si symmetric stretching, while the absorption peaks at  $1100\text{ cm}^{-1}$  and  $1230\text{ cm}^{-1}$  are assigned to asymmetric stretching of Si–O–Si. An absorption peak at  $960\text{ cm}^{-1}$  was found in both HTS-1 and MTS-1, which is considered to be a collective vibration of the Si–O–Ti bond or Si–O bond perturbed by the presence of tetrahedrally coordinated  $Ti^{4+}$  in the framework of HTS-1 zeolite.<sup>23,24</sup>

The morphology of samples synthesized by a dissolution-recrystallization process was investigated by TEM as shown in Fig. 2. Compared to the traditional TS-1 (Fig. 2A), the HTS-1 has many large voids, where located merely in the inner part of the crystals (Fig. 2B and 2C). It is also interesting to find that both the size and external shape of hollow TS-1 particles are very similar to those of the original zeolite, which indicates that the post-treatment affects essentially the core of the crystals and never communicates directly with the surface. The formation of voids in TS-1 cannot result from a Ti gradient concentration, but due to a gradient of defect sites throughout the crystals.<sup>25</sup> In catalytic reaction, this kind of hollow-structure avoids the shortage of traditional TS-1 (as shown in Table S1), which is important to decrease pore diffusion limitations and facilitate bulky molecular transport to catalytic sites and increasing the catalyst activity. Besides, the TEM results in Fig. 2D confirmed that manganese species in MTS-1 were highly dispersed into hollow-structured zeolite and the formation of framework Mn species for there not found any new external shape, which is similar to the results of UV–visible spectra and X-ray diffraction.

As shown in Fig. 3A, the XRD patterns indicate that the prepared materials are well crystallized, the diffraction peaks at  $7.95^\circ$ ,  $8.94^\circ$ ,  $23.2^\circ$ ,  $23.7^\circ$ ,  $24.1^\circ$  and  $24.9^\circ$  show that the catalysts possess a MFI-type structure.<sup>26</sup> Compared with silicate-1, the patterns of HTS-1 exhibited an additional diffraction peak at  $2\theta$  of  $25.56^\circ$ , indicating a change from a monoclinic symmetry to an orthorhombic symmetry.<sup>27</sup> After the Mn element incorporated, there weren't other phases to be founded by XRD characterization, which manifested that the post-treatment process did not change the MFI framework structure of HTS-1. In addition, no diffraction peaks corresponding to crystalline  $MnO_x$  clusters were detected, which indicates that the manganese element has been well-incorporated into the skeleton of molecular zeolite or homogeneously dispersed in molecular zeolite lattices.<sup>28</sup> Furthermore, compared with the standard phase of HTS-1, manganese-containing materials show a slight move of the diffraction peaks to a smaller angle, 1% MTS-1 ( $0.02^\circ$ ) and 5% MTS-1 ( $0.05^\circ$ ) (Fig. 3B). This is may be due to deduce substitution of smaller tetrahedrally coordinated Si atoms ( $0.4\text{ \AA}$  in crystal form) with heteroatom Mn having a larger size ( $0.5\text{--}1.0\text{ \AA}$ ) as ions in the crystalline environment, bringing about an increased lattice parameter value.

XPS analysis was utilized to detect both the surface concentration and chemical valence of elements present in the as-obtained MTS-1 (Fig. 4). The XPS survey spectrum reveals that the 5% Mn containing HTS-1 sample shown in Fig. 4A composed of the Ti, Mn, and O elements. The Mn 2p core level spectrum (Fig. 4B) indicates that the measured values of the binding energies (BE) for Mn  $2p_{3/2}$  and Mn  $2p_{1/2}$  ( $641.8$  and  $653.3$  eV, respectively) are in good

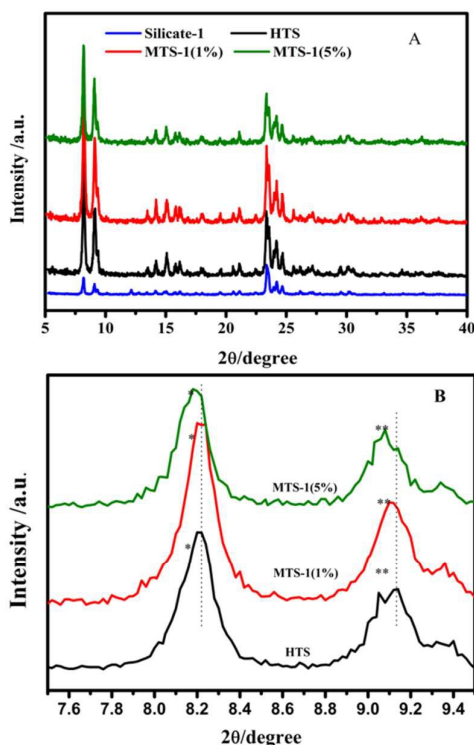


Fig. 3 Wide-angle XRD patterns (A) and enlarged scale between  $2\theta = 7.5^\circ$  and  $9.5^\circ$  of (B)

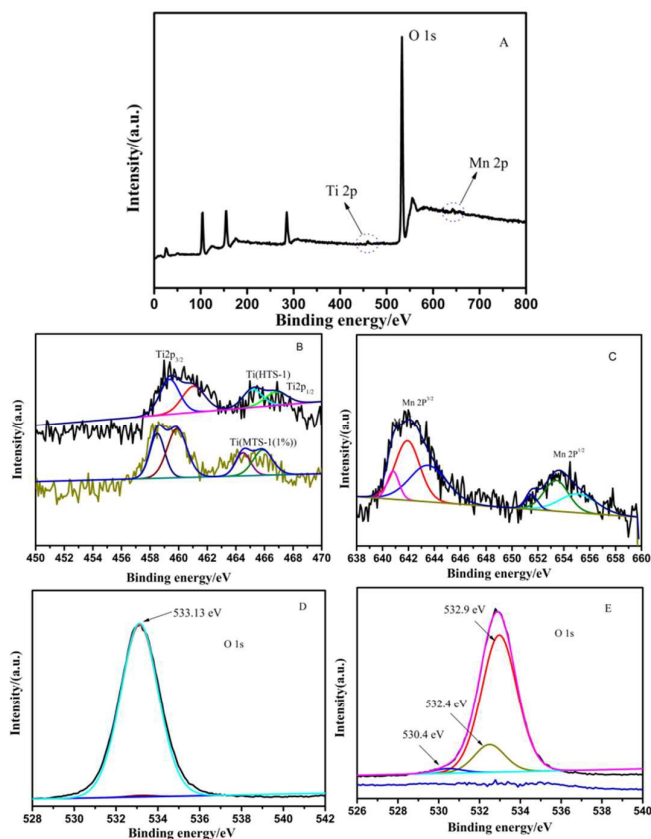


Fig. 4 XPS wide energy range (0–550 eV) survey scan of the xMTS-1 samples (A); Mn(2p) core level XPS of parent HTS-1 (B); Ti(2p) core level XPS (C); XPS spectra of O 1s region in HTS-1 (D); XPS spectra of O 1s region in MTS-1 (E).

accordance with the reported values for Mn (III or IV).<sup>29</sup> The core level spectra of Ti 2p in HTS-1 (Fig. 4C) showed the binding energies for Ti  $2p_{3/2}$  and Ti  $2p_{1/2}$  (458.8 eV and 464.3 eV, respectively). While after the Mn element doped, the curves moved slightly to a larger binding energy, which confirmed that the bond strength of Ti–O was tiny changed by the incorporation of manganese species.<sup>29</sup> Besides, the peak area ratio located at 460.0 eV belonged to tetrahedral Ti element, reduced with the doping of Mn species, demonstrating the formation of framework Mn–O–Si.<sup>30</sup> To further define the existence of a double active-site in MTS-1 framework, the O 1s core level spectrum of the HTS-1 and MTS-1 sample are shown in Fig. 4D and 4E. The binding energies of 533.13 eV shown in Fig. 4D is due to the O–Si and Ti–O type,<sup>31</sup> while two new binding energies of 530.4 eV and 532.4 eV are observed for MTS-1 in Fig. 4E. The BE of 530.4 eV can be assigned to a handful of Mn–O binding in  $\text{MnO}_2$ , and the BE of 532.4 eV belong to the Ti–(OSiO)<sub>4</sub>–Mn species.<sup>32</sup> This suggests that the most Mn species are incorporated into the HTS-1 framework.

$\text{N}_2$  adsorption-desorption analysis for TS-1, HTS-1 and the obtained MTS-1 are recorded in Fig. 5A. The adsorption-desorption

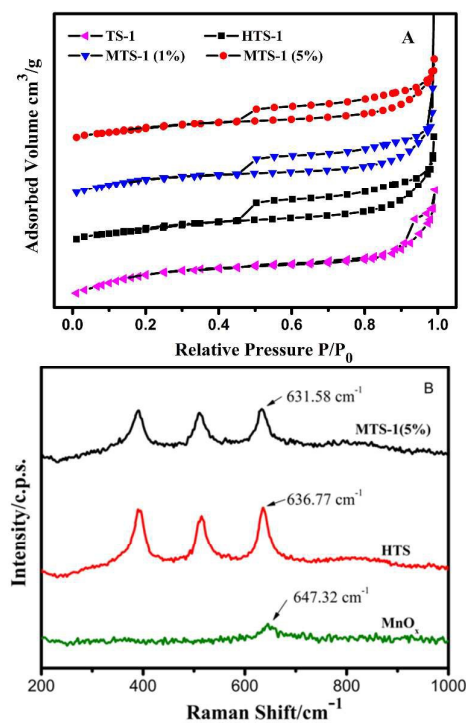


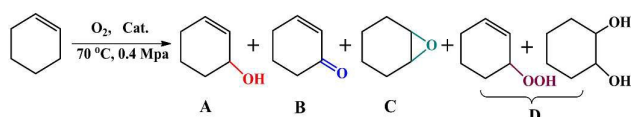
Fig. 5  $\text{N}_2$  adsorption-desorption isotherms (A) and Raman spectra (B) of samples

isotherms of traditional TS-1 indicates that there is no significant mesoporosity (hollow structure). But TS-1 via a dissolution-recrystallization process, shows that there are intra-crystalline voids and the size of entrance pores into these voids. This can be confirmed by an obvious large hysteresis loop from 0.43 to 0.99 (Fig. 5A),<sup>33</sup> which is primarily observed on porous zeolite crystals and mesoporous MCM-41 having extensive structural defect holes amid the channels.<sup>34</sup> A comparison of the surface areas of the three materials (Table S1) shows that HTS-1 has a surface area close to

traditional TS-1 (323 vs. 341 m<sup>2</sup>/g and 335 m<sup>2</sup>/g for 5% MTS-1). This comparison of surface areas indicated that the recrystallization process leads to a material that has a unique hollow structure, not a simple modification of the surface.

Raman is an effective technique which can detect slight phase information, e.g. framework metal sites in zeolite and extra-framework species. Thence Raman was utilized to detect the effect of implanting manganese in the framework of HTS-1 zeolite with excitation laser beams of 544 nm (Fig. 5B). A well-resolved peak was observed between 390 cm<sup>-1</sup> and 636 cm<sup>-1</sup> for the HTS-1 materials with or without manganese, which is assigned to the characteristic vibrations of the Si-O and Ti-O bonds in the five-membered ring of the MFI-type unit structure. The position of this peak shifted to the lower wave numbers (red shift) as the Mn species were implanted in HTS-1, which might be due to the asymmetric stretching vibration of the bending and symmetric stretching vibrations of framework Mn-O-Si.<sup>32</sup>

Under the investigated reaction conditions, the allylic oxidation of cyclohexene mainly produced 2-cyclohexen-1-ol (A), 2-cyclohexen-1-one (B), epoxycyclohexane (C) and other products including cyclohexenyl hydroperoxide and 1,2-cyclohexanediol (D) were detected in the reaction mixture, summarized as below.



Catalytic performances of various catalysts, including silicate-1, Mn-silicate-1 and MTS-1 are summarized in Table 1.

Table 1 Catalytic performances of the different catalysts

Entry	Catalyst	Conv.% <sup>a</sup>	Selectivity% <sup>b</sup>			
			A	B	C	Others
1	Blank	5.6	6.2	34.5	3.5	55.8
2	Silicate-1	5.5	6.1	36.2	3.8	53.9
3	Mn-Silicate-1	14.3	29.	60.2	3.5	6.8
4	MnO <sub>x</sub>	8.2	17.	46.2	3.1	33.0
5	TS-1	9.7	25.	37.8	2.8	34.1
6	HTS-1	12.2	29.	36.3	2.7	31.8
7	MTS-1(1%)	18.4	34.	57.6	3.2	5.0
8	MTS-1(5%)	25.4	31.	65.4	2.9	0.5
9	MTS-1(7%)	28.2	28.	62.3	3.9	4.9

Reaction conditions: 0.1 g of catalyst; 100 mmol of substrate; 0.4 MPa O<sub>2</sub>; 70 °C; 6 h. a: Cyclohexene conversion = (the amount (mmol) of cyclohexene before reaction – the amount (mmol) of cyclohexene after reaction) / the amount (mmol) of cyclohexene before reaction × 100%. b: Product selectivity = content of this product / content (mmol) of each product × 100%.

A blank experiment showed that the non-catalytic auto-oxidation of cyclohexene gave 5.6% conversion after 6 h. The Si species did not display any catalytic activity to the allylic oxidation of cyclohexene (entry 2). Compared to the silicate-1, traditional TS-1 exhibited a relatively higher catalytic activity (entry 5), which can be concluded that the skeleton Ti species is a key factor in zeolite. Obviously, the activity of the HTS is higher than traditional TS-1 (entries 5 and 6). The main reason for this difference can be attributed to that the hollow structure of HTS-1 can enhance the accessibility of the reactant molecules to active centers and the fast diffusion of

products,<sup>10</sup> which is consistent with the characterization analysis (measured from TEM). As shown in Table 1, MTS-1 displayed a higher activity for the allylic oxidation of cyclohexene. With the increase of Mn content, the conversion of cyclohexene increased constantly, while the selectivity of A and B increased first and then decreased. This may be due to that the framework Mn(III) as strong Lewis acid sites and highly active components can promote the decomposition of peroxide and the production of radicals •OH, thus accelerating the allylic oxidation of cyclohexene. By the aforesaid, we can infer that the structure of bimetal catalyst is benefit to the catalytic cycle.

Fig. 6A shows the variation of cyclohexene conversion and selectivity with the temperatures. With an increase of temperature from 60 °C to 100 °C, the conversion of cyclohexene increased from 8.2% to 35.4%. The selectivity of B increased from 41.7% to 64.7%, and then decreased to 52.7%, the selectivity of A decreased from 40.6% to 28.6%. However, the content of the others decreased from 15.2% to 0.5%, and then increased to 8.8%, which may be attributed to the increasing content of 1,2-cyclohexanediol by the hydrolysis of epoxycyclohexane. The effect of the amount of 5 wt% MTS-1 catalyst on the reaction was examined by varying the catalyst amount from 0.05 g to 0.3 g, while other reaction condition parameters were kept constant (Fig. 6B). The results showed that cyclohexene conversion and the selectivity of A and B increased almost linearly with the catalyst mass addition

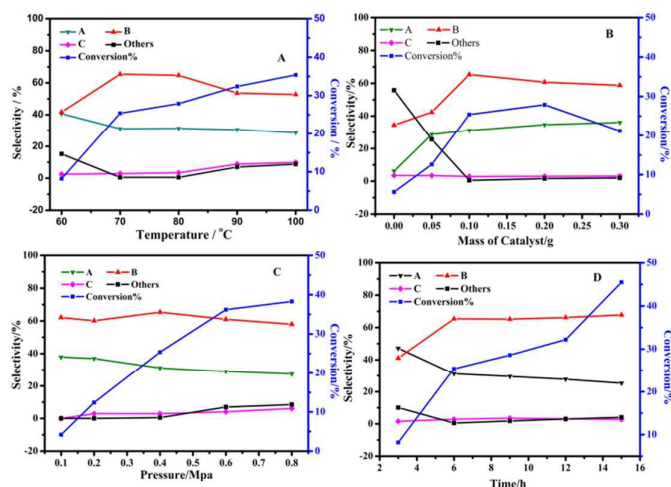


Fig. 6 Effect of various parameters

lower than 200 mg, where as the selectivity for cyclohexenyl hydroperoxide continuously decreased. This can be ascribed to the following factor: the Ti species induces the formation of cyclohexenyl hydroperoxide; while the Mn species could lead to the relatively faster decomposition of cyclohexenyl hydroperoxide to produce A and B. However, adding more catalyst led to a lower cyclohexene conversion. This phenomenon may be explained through that the transition metals in media of low polarity might act as catalyst at low loadings, but inhibitors at high loadings, as reported by Sheldon.<sup>35</sup> The effects of reaction pressure were checked and the results are shown in Fig. 6C. Cyclohexene conversion increased with the partial pressure of oxygen, which might be explained by better solubility of

oxygen in the reaction system. Further increasing the reaction pressure did not affect cyclohexene conversion too much; while no obvious change in the product distribution was observed. Fig. 6D displays the changes of conversion and selectivity with different reaction times at a temperature of 70 °C. The conversion rapidly increased with reaction time; it increased from 8.2% to 45.5%. The selectivity of A decreased with the reaction time. Meanwhile, the selectivity of B increased and then remained almost unchanging. This result should indicate that 2-cyclohexene-1-ol produced was apt to be oxidized to 2-cyclohexene-1-one.

From the context of a 'green' approach, the reusability of MTS-1 was investigated in the multiple sequential oxidation of cyclohexene with O<sub>2</sub>. After each run, the recycled catalyst was repeatedly washed by deionized water and ethanol, then dried at 100 °C over night. The catalytic results are shown in Figure 7A. Obviously, there was no significant decrease in both the conversion of cyclohexene and selectivities of allylic oxidation products after ten recycles, demonstrating its stability under the reaction conditions. Furthermore, the solid catalyst was removed from the reaction mixture by filtration during the hot conditions and the oxidation was allowed to proceed with the mother liquor (filtrate) under the same conditions. The conversion continued to increase at a much lower

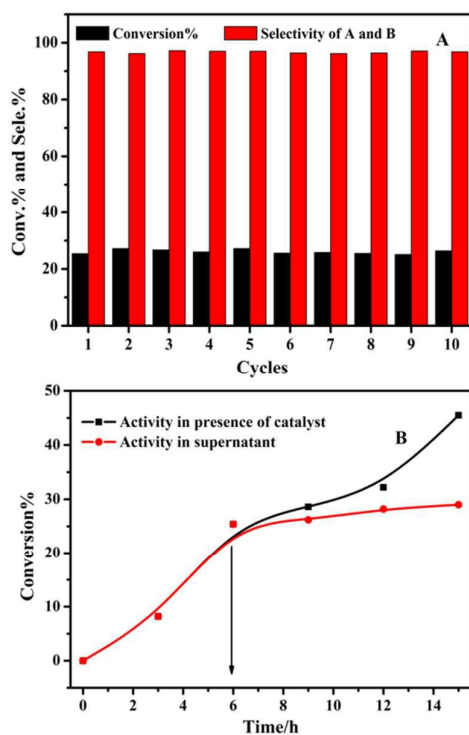


Fig. 7 Results of recycle (A) and hot-separation (B) test of 5% Mn-HTS catalyst

rate after the removal of the catalyst (Fig. 7B). The persistence of a low activity could be attributed to the thermal autoxidation, initiated by the oxygenated products, present in the mother liquor.<sup>36</sup> The leaching test was also carried out for Ti and Mn by ICP-AES analysis using the filtrate and it was found that no Ti or Mn ions were presented in the filtrate. Besides, the stability of MTS-1 was

also confirmed by comparison of XRD and UV-Vis spectra of the fresh and ten times reused (Fig. S2 in the ESI†). These results confirmed the catalytic behavior of MTS-1 as a truly heterogeneous catalyst during cyclohexene oxidation.

In summary, the new Mn-containing hollow TS-1 catalyst prepared by direct manganese incorporation into framework, exhibited an effective performance in the allylic oxidation of cyclohexene with O<sub>2</sub> under solvent-free conditions. The reusability of the catalyst which is a prerequisite for practical applications was analysed and it was found that the catalyst exhibits no significant changes in its catalytic activity even after ten cycles of reuse. This can be further strengthened by the fact that the use of a transition metal framework material could overcome leaching problems and benefit catalyst recycling. In addition, data shown in Table S2 compares the results obtained MTS-1 catalytic system and other systems used for this reaction. The present reported catalytic systems were simple, reusable and effective models for higher cyclohexene conversion with better product selectivity. Therefore, in terms of green chemistry, these catalysts may open a new avenue for hydrocarbons oxidation with molecular oxygen.

## Notes and references

- G. Cainelli and G. Cardillo, *Chromium Oxidations in Organic Chemistry*; Springer-Verlag: Berlin, 1984.
- Y. Cao, H. Yu, F. Peng, and H. Wang, *ACS Catal.*, 2014, **4**, 1617–1625.
- K. Leus, G. Vanhaelewyn, T. Bogaerts, Y. Y. Liu, D. Esquivel, F. Callens, G. B. Marin, V. Van Speybroeck, H. Vrielinck and P. Van Der Voort, *Catal. Today*, 2013, **208**, 97–105.
- D. Jiang, T. Mallat, D. M. Meier, A. Urakawa and A. Baiker, *J. Catal.*, 2010, **270**, 26–33.
- J. Hao, X. Jiao, L. Han, Q. Suo, A. Ma, J. Liu, X. Lian and L. Zhang, *RSC Adv.*, 2015, **5**, 13809–13817.
- A. Dali, I. Rekkab-Hammoumraoui, A. Choukchou-Braham and R. Bachir, *RSC Adv.*, 2015, **5**, 29167–29178.
- A. Corma, *Chem. Rev.*, 1997, **97**, 2373–2420.
- Y. Tao, H. Kanoh, L. Abrams, K. and Kaneko, *Chem. Rev.*, 2006, **106**, 896–910.
- L. H. Chen, X. Y. Li, G. Tian, Y. Li, J. C. Rooke, G. S. Zhu, S. L. Qiu, X. Y. Yang and B. L. Su, *Angew. Chem. Int. Ed.*, 2011, **50**, 11156–11161.
- Y. Ko, S. J. Kim, M. H. Kim, J.-H. Park, J. B. Parise and Y. S. Uh, *Micropor. Mesopor. Mat.*, 1999, **30**, 213–218.
- U. Wilkenhöner, G. Langhendries, F. van Laar, G. V. Baron, D. W. Gammon, P. A. Jacobs and E. van Steen, *J. Catal.*, 2001, **203**, 201–212.
- P. Ratnasamy, D. Srinivas, and H. Knözinger, *Adv. Catal.*, 2004, **48**, 1–169.
- Y. Goa, P. Wu and T. Tatsumi, *J. Phys. Chem. B*, 2004, **108**, 8401–8411.
- E. V. Spinace, H. O. Pastore and U. Schuchardt, *J. Catal.*, 1995, **157**, 631–635.
- Y. Meng, H. C. Genuino, C.-H. Kuo, H. Huang, S.-Y. Chen, L. Zhang, A. Rossi and S. L. Suib, *J. Am. Chem. Soc.*, 2013, **135**, 8594–8605.
- W. S. Kijlstra, E. K. Poels, A. Bliet, B. M. Weckhuysen and R. A. Schoonheydt, *J. Phys. Chem. B*, 1997, **101**, 309–316.
- D. Radu, P. Glatael, A. Gloter, O. Stephan, B. M. Weckhuysen and F. M. F. de Groot, *J. Phys. Chem. C*, 2008, **112**, 12409–12416.

- 18 Y. Wang, M. Lin and A. Tuel, *Microporous Mesoporous Mater.*, 2007, **102**, 80–85.
- 19 S. Bordiga, F. Bonino, A. Damin and C. Lamberti, *Phys. Chem. Chem. Phys.*, 2007, **9**, 4854–4878.
- 20 H. Liu, G. Lu, Y. Guo and Y. Guo, *Appl. Catal. A*, 2005, **293**, 153–161.
- 21 D. M. Sherman, *Phys. Chem. Miner.*, 1987, **14**, 355–363.
- 22 K. Langer, A. N. Platonov, S. S. Matsyuk and M. Wildner, *Eur. J. Mineral.*, 2002, **14**, 1027–1032.
- 23 A. Kumar, D. Srinivas and P. Ratnasamy, *Chem. Commun.*, 2009, 42, 6484–6486.
- 24 G. Ricchiardi, A. Damin, S. Bordiga, C. Lamberti, G. Spanò, Frivetti and A. Zecchina, *J. Am. Chem. Soc.*, 2001, **123**, 11409–11419.
- 25 J. R. Agger, N. Hanif and M. W. Anderson, *Angew. Chem. Int. Ed.*, 2001, **40**, 4065–4067.
- 26 X. Ke, L. Xu, C. Zeng, L. Zhang and N. Xu, *Micropor. Mesopor. Mat.*, 2007, **106**, 68–75.
- 27 Y. Li, Y. Lee and J. Porter, *J. Mater. Sci.*, 2002, **37**, 1959–1965.
- 28 W.-S. Lee, M. C. Akatay, E. A. Stach, F. H. Ribeiro and W. N. Delgass, *J. Catal.*, 2012, **287**, 178–189.
- 29 M. Kang and M.-H. Lee, *Appl. Catal. A*, 2005, **284**, 215–222.
- 30 Y. Xu, B. Lei, L. Guo, W. Zhou and Y. Liu, *J. Hazard. Mater.*, 2008, **160**, 78–82.
- 31 S. Contarini, P. V. der Heide, A. Prakash and L. Kevan, *J. Electron Spectrosc.*, 2002, **125**, 25–33.
- 32 L. Jin, L. Xu, C. Morein, C. Chen, M. Lai, S. Dharmarathna, A. Doble and S. L. Suib, *Adv. Funct. Mater.*, 2010, **20**, 3373–3382.
- 33 Y. Wang and A. Tuel, *Micropor. Mesopor. Mater.*, 2008, **113**, 286–295.
- 34 H.-P. Lin, S.-T. Wong, C.-Y. Mou and C.-Y. Tang, *J. Phys. Chem. B*, 2000, **104**, 8967–8975.
- 35 J. H. Tong, Y. Zhang, Z. Li and C. G. Xia, *J. Mol. Catal. A: Chem.*, 2006, **249**, 47–52.
- 36 Z. Cai, M. Zhu, J. Chen, Y. Shen, J. Zhao, Y. Tang and X. Chen, *Catal. Commun.*, 2010, **12**, 197–201.

